3. Formulation and optimization of abciximab coated mesoporous silica nanoparticles for improved antithrombotic activity

3.1 Objective

The objective of this study to prepare ABX decorated MSN and characterized their physicochemical properties such as shape, particle size, zeta-potential. surface morphology and surface chemistry, *in-vitro*, hemocompatibility in human blood, *in-vivo* bleeding time, clotting time, and antithrombotic $FeCl_3$ model assay.

3.2 Plan of study

a. Preparation and optimization of MSN-NH_2

b. Preparation of ABX coated MSN

c. Physicochemical and *in-vitro* evaluation of synthesized nanoparticles

- Particle size, polydispersity index and zeta potential by DLS
- Determination of entrapment efficiency
- Electron microscopy (SEM, TEM & SAED)
- Degree of peptide conjugation by Bradford Assay
- Surface chemistry by XPS
- Crystallographic studies by XRD
- Physical stability by TGA
- *In-vitro* drug release studies
- *In-vitro* blood clot assay
- Biocompatibility and safety evaluation
- *In-vitro* clot targeting efficiency by platelet binding
- Serum Stability Studies

d. *In-vivo* evaluation of synthesized nanoparticles

- Tail bleeding assay in Swiss Albino mice

- Blood clotting time study in Swiss Albino mice
- $FeCl_3$-induced thrombosis model

3.3. Materials

Abciximab injection was obtained from Reliance life sciences Pvt. Ltd, Navi Mumbai, India. Cetyltrimethylammonium bromide (CTAB, 99 %) was acquired from S D Fine chemicals, Mumbai, India. Thrombin from bovine plasma, fibrinogen from human plasma, and (3 aminopropyl) trimethoxysilane (APTES) were procured from Sigma Aldrich St. Louis, USA. Tetraethyl orthosilicate (TEOS, 98 %), dimethyl sulfoxide (DMSO), methanol (HPLC grade), and Bradford reagent for proteins were obtained from Sisco research laboratories Pvt. Ltd., India. DiD dye was purchased from Thermo fisher scientifc, USA. Wright-Giemsa stain was procured from Labogenes, India. Phosphate buffered saline (PBS) pH 7.4 was purchased from Himedia Laboratories Pvt. Ltd. Mumbai, India. Sodium hydroxide was obtained from Loba Chemie, Mumbai, India. Hydrochloric acid was acquired from Merck life science Pvt. Ltd., India. Millipore water was used from a LAB-JAL Milli-Q System (Lab India instrument Pvt. Ltd.). All other chemicals used were of analytical grade.

3.4. Methods

3.4.1. Selection of CMAs and CQAs

Preliminary studies were conducted to identify the important quality attributes of the gene rated system on the basis of the required quality product profile. Particle size was selected as one of the Critical Quality Attributes (CQAs) because a smaller size enhances the surface area and is capable to avoid the RES uptake. The PDI was further selected as a CQA because the monodispersity of particles can later decide the fate of drug release. Critical Material Attributes (CMAs) were also selected among several material attributes based on a literature survey [175].

3.4.1.1. Formulation optimization by Box-Behnken Design (Randomized)

Numerical and graphical optimization of mesoporous silica nanoparticles was performed to establish an optimized batch by using Box-Behken design. CTAB concentration (0.25-1 %w/v), TEOS concentration (2.5-5 mL), and APTES concentration (0.25-0.75 mL) were used as independent variables to study the effect on formulation characteristics, i.e., particle size, and PDI (response variable), during the optimization of the formulation as shown in **Table 3.1**. There was a total of 15 batches in the design space representing 3 center points and 12 axial points mentioned in **Table 3.3**.

Table 3.1. Box-Behnken design of MSN explaining different variables by Design Expert version 11 (Trial)

Independent variables	**Levels**		
	-1	0	+1
X1= Conc. of CTAB (in %w/v)	0.25	0.62	1.00
X2= Conc. of TEOS (in mL)	2.50	3.75	5.00
X3= Conc. of APTES (in mL)	0.25	0.50	0.75
Dependent variables or Response	**Constraints**		
Y1= Particle size	Minimize		
Y2= PDI	Minimize		

3.4.2. Preparation of amino-functionalized MSN (MSN-NH_2)

The previously described method with little modification was used for the preparation of MSN- NH_2. In brief, 200 mL of CTAB aqueous solution (0.25 % w/v) was prepared, and then 1.75 mL of 2 M NaOH solution was mixed in dropwise manner with vigorous stirring at 80 ◦C for 20 min. Further, 2.5 mL TEOS was gently introduced to the aforesaid mixture under vigorous stirring to obtain the resultant clear liquid. Thereafter, 0.5 mL of APTES was gently added, and the temperature of the reaction mixture was maintained at 80 ◦C for the next 2 h under vigorous stirring [176]. The white precipitate was recovered after centrifuging for 10 min at 8000 rpm and washing in triplicate with Millipore water. The surplus CTAB surfactant template was extracted by refluxing it for 10 h at 80 ◦C in a

mixture of hydrochloric acid (9 mL, 37 % v/v) and methanol (150 mL). Subsequently, the resulting mixture was centrifuged and rinsed twice with millipore water and methanol. The resulting MSN-NH_2 solid powder was then dried at 50 ◦C under vacuum [89]. The scheme of formulating MSN-NH_2 has been presented in **Figure. 3.1 A.**

3.4.3. Conjugation of ABX to MSN- NH_2

The prepared MSN-NH_2 nanoparticles (10 mg/mL) were dispersed in PBS 7.4 pH by ultrasonication and were incubated for 3 h with the ABX (2mg/mL). The attachment of ABX on MSN-NH_2 was achieved by the direct conjugation of antibodies by electrostatic interaction. The negatively charged ABX conjugated over the surface of cationic charged MSN-NH_2 through electrostatic interactions. The unconjugated ABX was drawn out by centrifugation at 10,000 rpm and the pellet of the nanoparticles was collected and redispersed in the phosphate buffer saline 7.4 pH [177]. The scheme of formulating MSN-NH_2 has been presented in **Figure. 3.1B**. The contents of different batches have been presented in **Table 3.2**

3.4.4. Preparation of DiD dye loaded ABX coated MSN-NH_2

All the batches of nanoparticles (DiD-MSN-NH_2 and DiD-MSN-ABX) were prepared with the previously mentioned techniques with little modifications. The 100 µg of DiD dye solution in dimethyl sulfoxide (1 mg/mL) was incubated with previously prepared MSN-NH_2 and MSN-ABX (10 mg/mL) for 24 h at room temperature with continuous stirring in the dark. The unloaded dye was then removed by centrifugation (8000 rpm, 10 min) and examined for % entrapment efficiency by indirect method [178]. The amount of DiD content in the supernatant (unloaded) was measured by fluorescence spectroscopy at excitation λ = 644 nm and emission λ = 665 nm. The entrapment efficiency was then calculated by using the following equation:

$$\%Entrapment\ efficiency = \frac{Total\ ammount\ of\ DiD\ added - ammount\ of\ Did\ in\ supernatant}{Total\ ammount\ of\ DiD\ added} \times 100$$

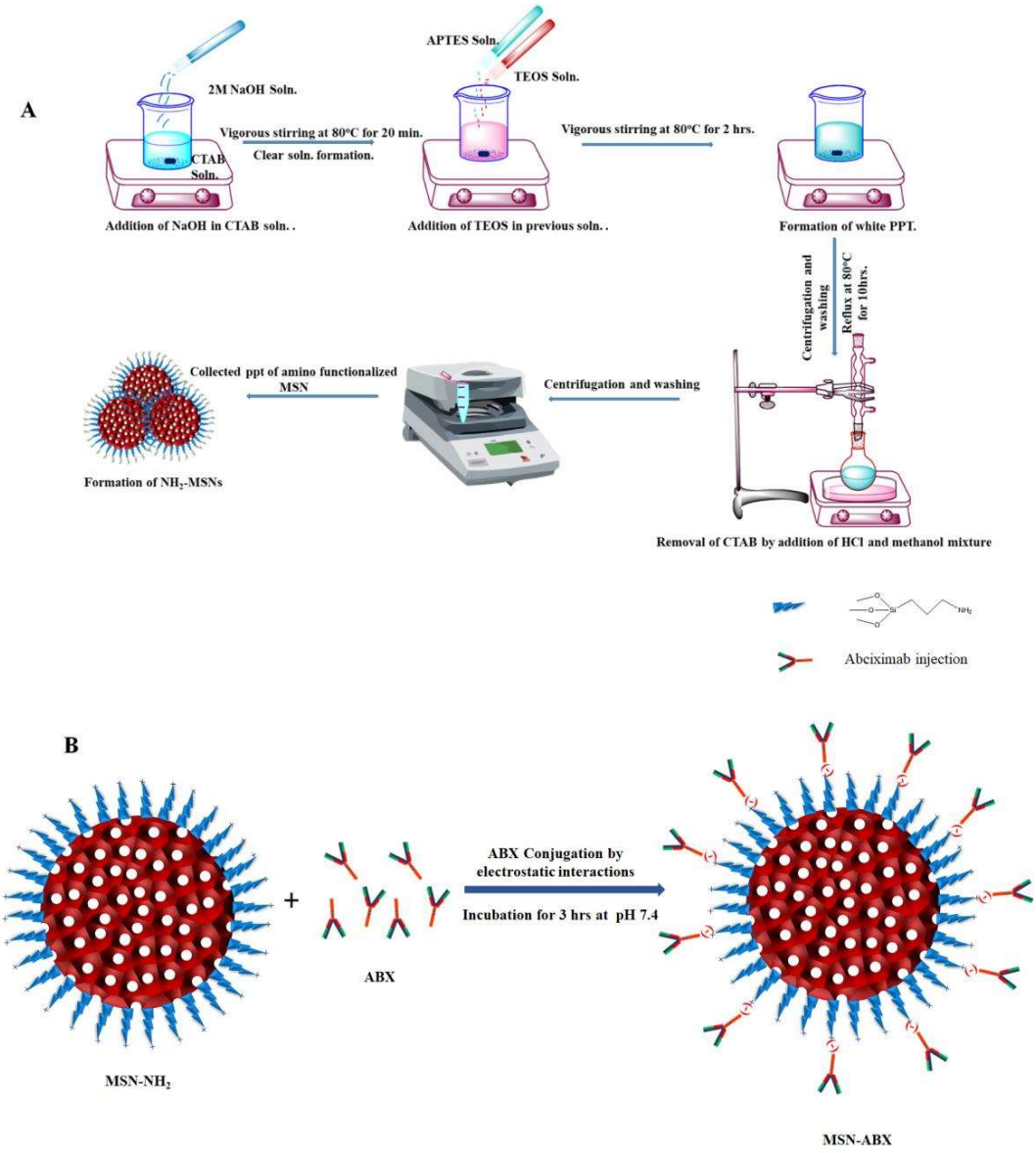

Figure 3.1. Graphical illustration of the preparation method of functionalized MSN. (A) synthesis of MSN-NH_2 (B) ABX functionalization of MSN-NH_2 by ionic interaction

Table 3.2. Formula of non-targeted and ABX decorated MSN

Batches	CTAB (mg)	TEOS (mL)	APTES (mL)	ABX (mg)	DiD dye (µg)
MSN-NH_2	500	2.5	0.5	-	
MSN-ABX	500	2.5	0.5	2	
DiD-MSN-NH_2	500	2.5	0.5	-	100
DiD-MSN-ABX	500	2.5	0.5	2	100

MSN-NH_2: Amino functionalized mesoporous silica nanoparticles
MSN-ABX: Abciximab decorated mesoporous silica nanoparticles
CTAB: Cetyltrimethylammonium bromide
TEOS: Tetraethyl orthosilicate
APTES: (3-Aminopropyl) triethoxysilane
ABX: Abciximab injection

3.4.5. Nanoparticle characterizations

3.4.5.1. Particle size, polydispersity and zeta potential of nanoparticles

Particle size, polydispersity, and surface charge of MSN-NH_2 and MSN-ABX nanoparticles were investigated at room temperature by using the Malvern Zetasizer Pro, which works on the principle of dynamic light scattering technique. For each sample, the reported values are the average of three runs and all the studies were performed at pH 7.4 [179].

3.4.5.2. TEM analysis

The internal constitution and morphology of non-targeted (MSN-NH_2) and targeted (MSN-ABX) nanoparticles were examined by TEM (Tecnai G2 20 TWIN, FEI Company, USA) analysis. After being diluted ten times in millipore water, both the MSN formulations were sonicated for 5 min. One drop of each diluted sample was deposited at the TEM grids, vacuum dried for 24 h and then images were captured by using TEM [180]. The surface area electron diffraction (SAED) pattern was also analyzed to investigate the crystallinity of samples.

3.4.5.3. SEM analysis

Scanning electron microscopy was used to examine the surface morphology of non-targeted and targeted MSN (Nova Nano SEM 450, USA (S.E.A.) PTE, Ltd.). Images were captured at a voltage of 20 kV with a magnification of 50 KX. The samples were prepared by diluting the nanoparticle formulations with millipore water, and a drop of each was mounted on the glass slides (1×1 cm) and dried overnight by maintaining the temperature 40 ◦C in a hot air oven. Carbon coating was applied to the coverslips before they were subjected to SEM imaging [181].

3.4.5.4. Surface chemistry

The surface chemistry of MSN-NH_2 and MSN-ABX were examined by using X-ray photoelectron spectroscopy (K-Alpha, Thermo Fisher Scientific) between 100 and 700 eV of binding energy. The sample was prepared by placing a drop of concentrated nanoparticle formulations on a glass slide and dried in a vacuum dryer overnight and the resulting samples were examined for XPS analysis [182].

3.4.5.5. XRD analysis

It was used to investigate crystallinity and related modification in physical state after being formulated into nanoparticles. Furthermore, this study was used to examine the purity of the components of the sample. The X-Ray diffraction system, Rigaku, Japan was employed to acquire the XRD spectra of MSN-NH_2. The diffractograms were captured at 2Θ angle ranges from 10◦ to 80◦ by using Ni filtered Cu Kα as a source of radiation and 10◦ /min scan speed was used with 40Kv tube voltage [183].

3.4.5.6. Thermogravimetric analysis (TGA)

The thermal stability and decomposition of MSN-NH_2 were determined by using TGA (Shimadzu, Japan). The weight of the initial sample was 2.47 mg in dried form. TGA data of the sample was collected at a heating range of 25−800 °C. The standard flow rate of N_2

was maintained during the experiment, and the heating increment rate was at 10 °C/min [184, 185].

3.4.5.7. Degree of ABX conjugation

Bradford assay was used to assess the degree of ABX conjugation to the surface of MSN [171, 186]. For the same, 1000 µl of nanoparticle formulation MSN-ABX (10 mg/mL), blank PBS pH 7.4, and ABX (equivalent concentration 2 mg/mL that was added initially) were treated in the dark with 5000 µl of the Bradford reagent. After 10 min samples were analyzed by UV spectroscopy. The ABX content over the surface of MSN-ABX was then calculated using the standard curve of bovine serum albumin (BSA) [174]. The following equation can be used to determine the extent of ABX conjugation:

$$\text{Degree of conjugation}(\%) = \frac{[\text{ABX Content in targeted NP-ABX Content in blank (PBS)}]}{\text{Content of standard ABX solution}} \text{X } 100$$

3.4.5.8. In-vitro characterization

3.4.5.8.1. In-vitro-ABX release

The ABX release profile among the targeted MSN at the physiological pH was determined by the sample separation method (**Figure 3.2**). The 3 mg/mL targeted MSN was placed in PBS (10 mL, pH 7.4) and maintained at 37 ± 0.5 ◦C under constant shaking. At a specified time schedule, 1000 µL of the sample was collected and centrifuged to separate both nanoparticles and supernatant. The aliquot volume was replaced with a fresh release medium after each sampling. Bradford assay was used to assess the amount of ABX released in the supernatant, and a graph showing cumulative percent drug release against time was prepared [187].

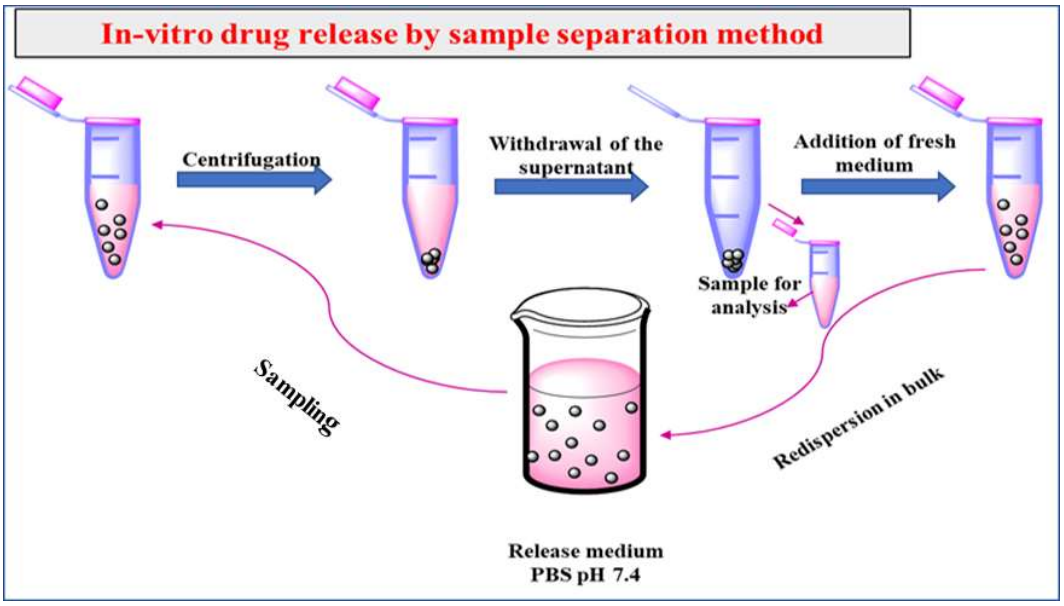

Figure 3.2. *In-vitro* drug release by the sample separation technique

3.4.5.8.2. In-vitro blood clot assay

The blood clot assay was carried out as the previously described method, with certain modifications presented in **Figure 3.3**. Before coagulation, 300 µl of blood was obtained through vein puncture from healthy human volunteers and immediately incubated for 1 h at 37 ◦C with 200 µl of 2 mg/mL ABX as a positive control, 200 µl of PBS, and 200 µl of MSN-ABX equivalent to 2 mg/mL of ABX in PBS 7.4. The resulted clot of the treated samples was weighed and compared [188].

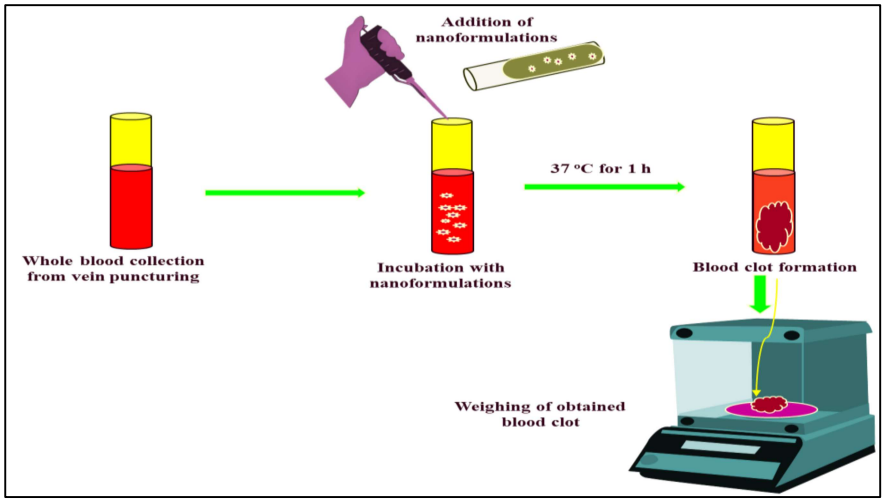

Figure 3.3. *In-vitro* drug blood clot assay

3.4.5.9. In-vitro clot targeting efficiency

3.4.5.9.1. In-vitro platelet binding assay by imaging through photon imager optima

This study was designed to evaluate the affinity of prepared nanoparticles towards activated platelets in both ways qualitatively and quantitatively. *In-vitro* clot targeting efficiency of MSN-ABX towards activated platelets was determined by an imaging system (photon imager optima, Biospace lab, France), a method had been presented in **Figure 3.4**. For the same MSN-ABX was incubated with the DiD dye for 24 h with stirring and the unloaded dye was removed by centrifugation at 6000 rpm. The platelets were isolated from the blood of the healthy human volunteers and washing was performed with normal saline then it was transferred to the glass vials. Further, 20 µl of 10 mg/mL fibrinogen with 10 µl of 10 U/mL of thrombin was added to the vials for initiation of the platelets activation process. Simultaneously PBS, DiD dye, DiD-MSN-NH_2, and DiD-MSN-ABX were added to the vials and incubated for 1 h. Afterward, the above setup was centrifuged at 6000 rpm for 10 min and the supernatant was removed. The resulting pellet of the cells was redispersed with 5 mL PBS (pH 7.4) and the above setup was placed in the imaging system. The fluorescent intensity of test vials was compared with the control and vials with standard concentrations of dye at the excitation and emission wavelength at 644 nm and 665 nm respectively [189, 190]. The 5 µg/mL in PBS 7.4 concentration of DiD dye was taken as standard and nanoparticles samples containing equivalent concentration of dye were used for the interaction study.

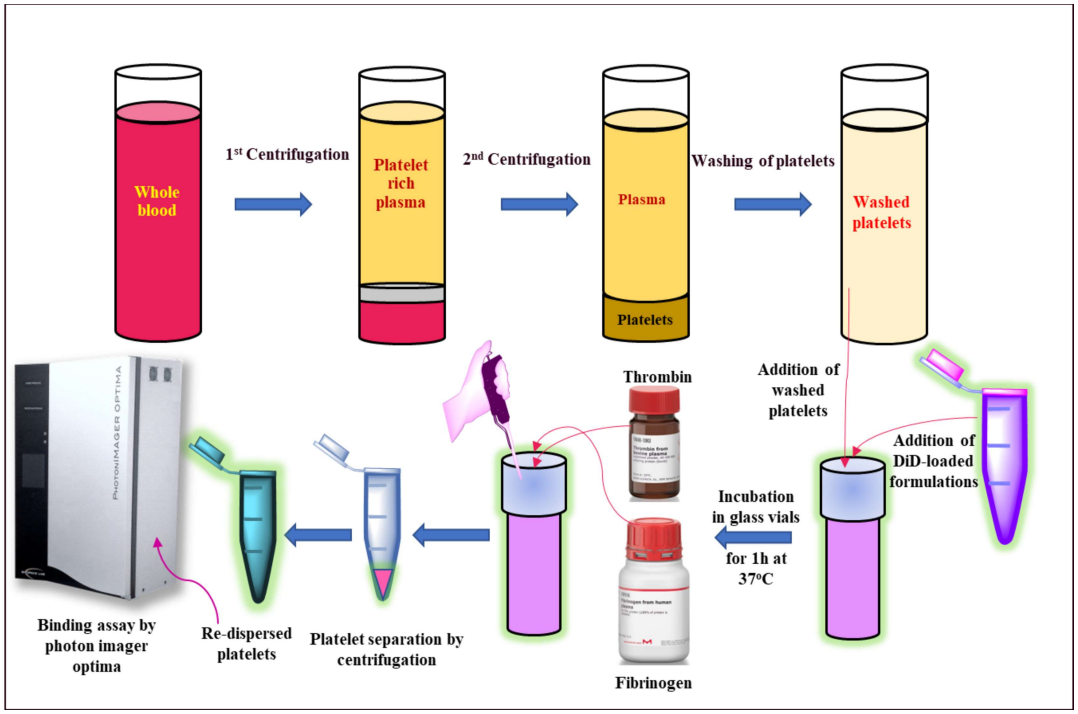

Figure 3.4. Graphical illustration of *in-vitro* imaging by photon imager optima

3.4.5.9.1. Image-J analysis of confocal laser microscopic images

The activated platelets were incubated for an hour with different DiD dye loaded formulations (MSN-NH_2 or MSN-ABX, 100 µL of 10 mg/mL) and then fixed by using 4 % paraformaldehyde in a cell concentration of 3×10^7. The cells were washed three times with PBS 7.4 pH to remove extra non interacted nanoparticles. The extent of red channels in fluorescent images of activated platelets after treatment was used to estimate the *in-vitro* clot targeting efficacy of DiD dye, DiD-MSN-NH_2, and DiD-MSN-ABX towards activated platelets. Image-J software was used to quantify the red channels of fluorescent images. The proportion of dark area was calculated when the fluorescent images were converted to binary black and white images [171, 190], the method had been presented in **Figure 3.5**.

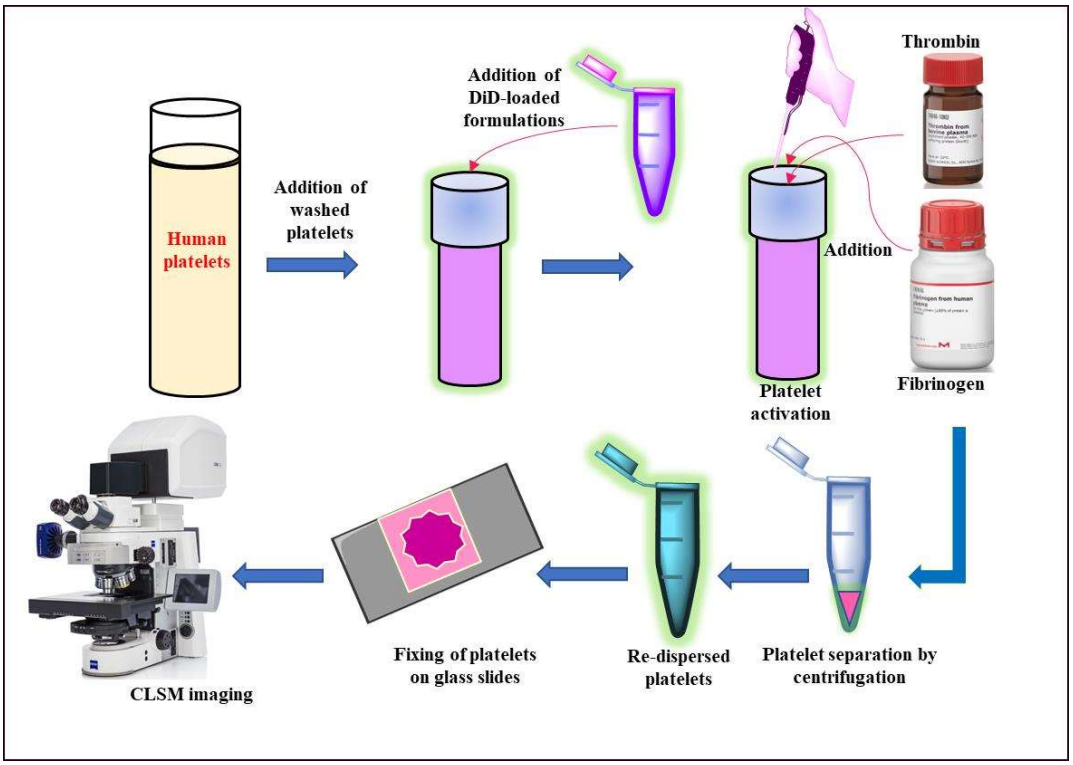

Figure 3.5. Graphical representation of *in-vitro* imaging by CLSM

3.4.5.10. In-vitro safety assessment

3.4.5.10.1. Blood Smear

Following the vein puncturing 5 mL of blood was collected from healthy human subjects. Further, 100 µl of 2 mg/mL ABX as a positive control, 200 µL of PBS, and 200 µL of MSN-ABX were incubated at 4 ◦C for 24 h. On the glass slides, a drop of the resultant blood mixture was placed and dispersed. All blood smears were prepared (triplicate) according to standard protocols, with Wright-Giemsa stain in methanol and successively rinsed with PBS (pH 7.4). After air drying, the produced blood smear was examined under a bright microscope to study the morphological changes in blood components including red blood cells, platelets, and white blood cells [12], presented in **Figure 3.6**.

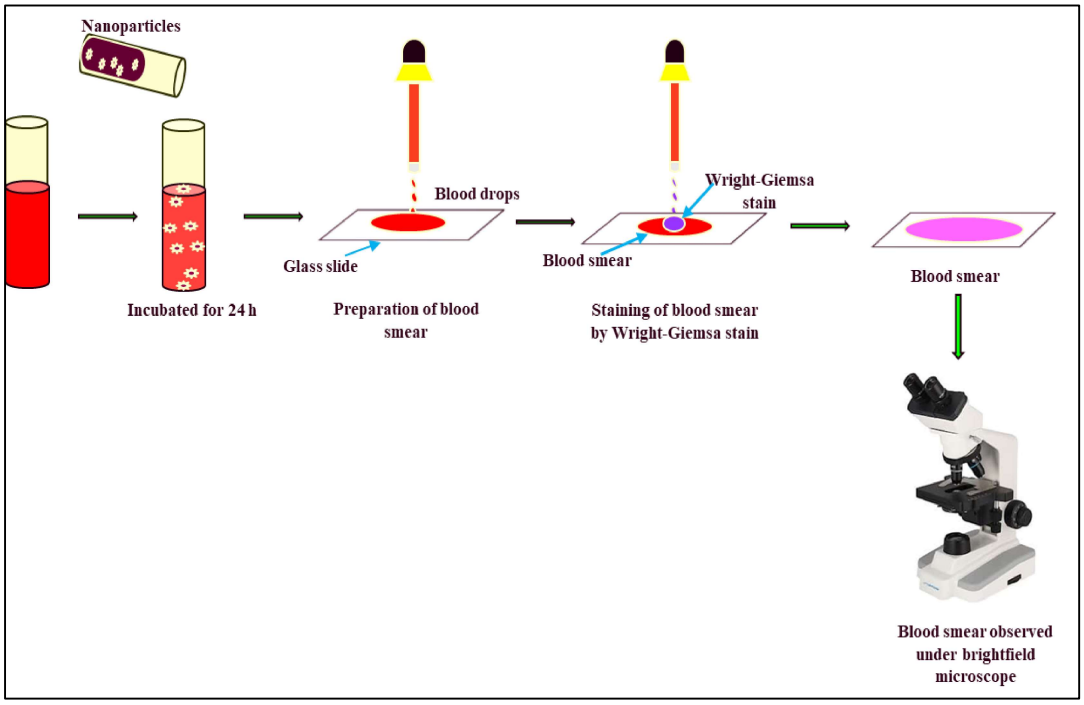

Figure 3.6. Schematic representation of blood smear preparation and analysis

3.4.5.10.2. Hemolytic Assay

Hemolytic analysis was performed to check the safety of ABX injections, non-targeted MSN, and targeted MSN in the blood of healthy subjects, shown in **Figure 3.7**. The plasma was recovered by centrifugation and sediment red blood cells were subsequently rinsed thrice with PBS. The mixture containing 0.2 mL (2 % v/v in PBS) of washed blood and 0.8 mL of nanoparticles (diluted in PBS) was then incubated for 2 h with moderate shaking for 30 min in an Eppendorf microtube. Following incubation, the solution was centrifuged for 10 min at 2000 rpm. The supernatant was then poured into the 96-well plate at a volume of 100 µl. The absorbance was measured at 570 nm, which was reported as the maximum absorption wavelength. The positive control taken was distilled water, whereas the negative control was PBS. The percentage of the hemolysis was determined by the following equation:

$$\%\text{Hemolysis} = [(\text{Abs T} - \text{Abs C})/(\text{Abs}100\% - \text{Abs C}) \text{ X } 100]$$

Here Abs T is the supernatant absorbance of the particles-incubated samples, Abs C is the negative control supernatant (PBS) absorbance, and Abs100% is the positive control supernatant absorbance [191].

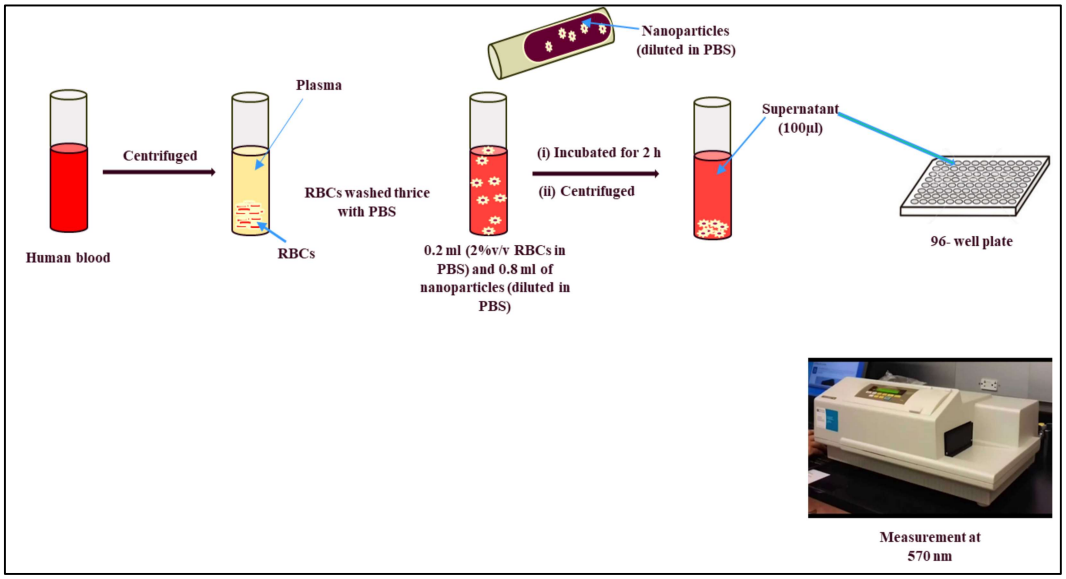

Figure 3.7. Schematic illustration of a method of hemolysis study

4.4.5. In vivo studies

4.4.5.1. Tail bleeding assay

Animal bleeding times are measured primarily to assess the hemorrhagic properties of antithrombotic medications. Nine male Swiss albino mice weighing about 20 ± 2 g were selected for the study and divided into 3 groups (n = 3). The age of the selected animals was 5−7 weeks. The saline, ABX, and MSN-ABX suspensions were administered (2mg/kg of ABX) by tail vein injection. The concentration of ABX was similar in all the batches. As for saline, the volume was kept equal. Further, the mice were anesthetized and kept on the heating table (37 °C) in the supine position. After completion of the latent period (1 h), the tail of the mice was transected with the surgical blade at a 1 cm distance from the tail tip. Instantly, after transection, the tail was dipped in the tube filled with saline (50 mL). The time was recorded up to the time until the bleeding stopped and was noted as bleeding

time. The maximum observation was done for 400 sec [192, 193]. A pictorial representation of a method of tail bleeding assay had been shown in **Figure 3.8**.

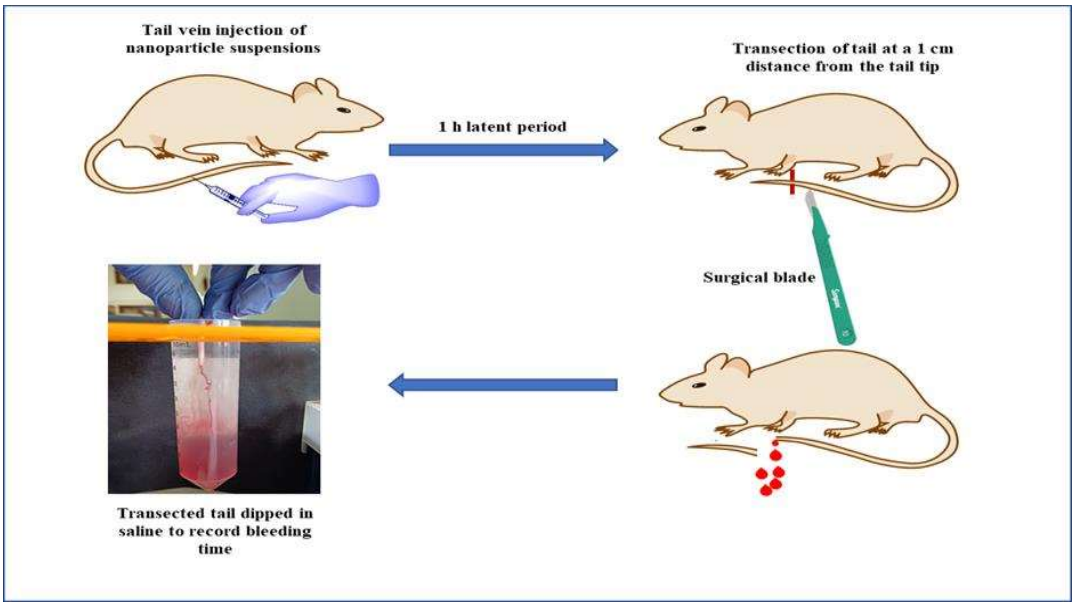

Figure 3.8. Pictorial representation of a method of tail bleeding assay

4.4.5.2. Blood clotting time study

Blood clotting time was measured as previously reported, presented in **Figure 3.9**. Briefly, the saline, ABX, and MSN-ABX were administered at a dose of 2 mg/kg of ABX (equal volumes of saline were used) through the tail vein. The tail of the mice was transected at the tip with the help of a surgical blade after 1 h of intravenous administration. The 25 µL of blood was collected in a microhematocrit capillary tube. The blood flow was allowed within the capillary by tilting it at an angle of 60° in up and down directions. The stopwatch was started at the point of blood contact with the capillary tube. The clotting time was reported as the blood ceased to flow in the capillary with the horizontal plane [194].

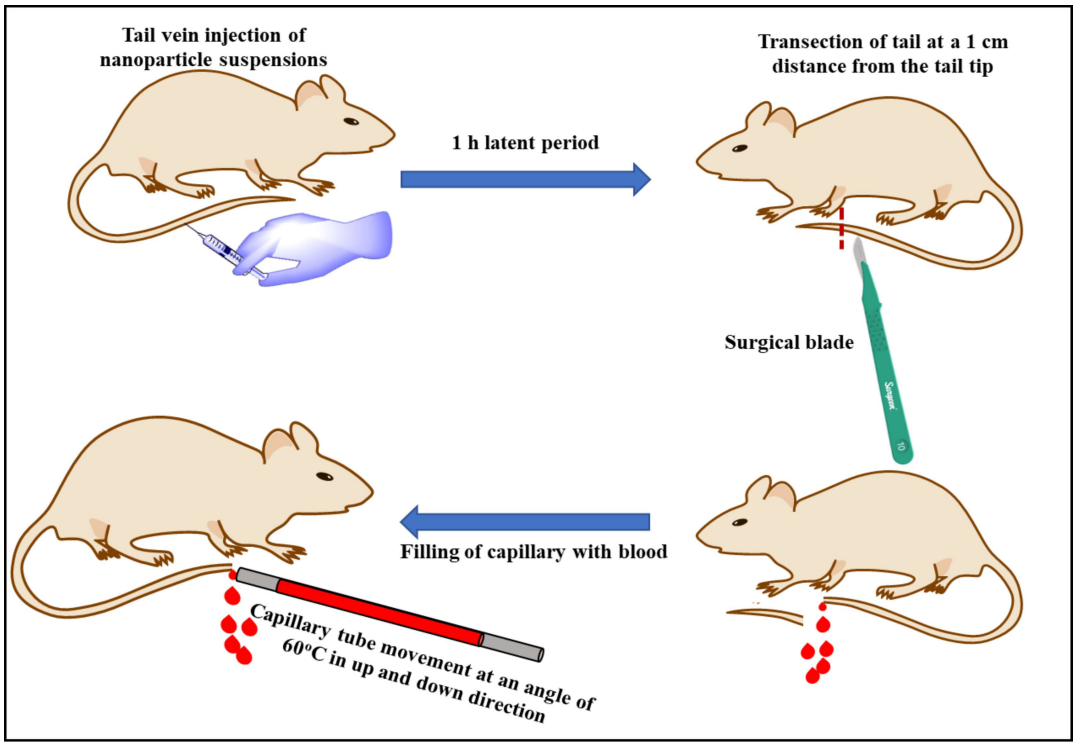

Figure 3.9. Graphical representation of method of *in-vivo* clotting time study

4.4.5.3. In-vivo $FeCl_3$ induced model for thrombus formation by B.P. measurement

Male Sprague Dawley rats weighing about 200 ± 20 g were kept in the animal house at room temperature of 25 ± 2 °C. Food and water were provided ad libitum (Hindustan Liver Ltd.). A modified version of blood pressure measurement was used in which invasive direct BP was recorded [195]. Rats were anesthetized by i.p injection of urethane (1.5 g/kg) and placed on a heat controllable table to prevent hypothermia. The midline cervical incision was performed to expose the carotid artery and was separated from the vagus nerve, the steps had been presented in **Figure 3.10 A**. Later, proximal cannulation of the carotid artery was performed for the direct measurement of blood pressure by PowerLab, AD Instruments, Australia. The intravenous tail vein injection of saline, ABX, and MSN-ABX at a dose of 2 mg/kg of ABX was administered to the anesthetized rat. As for saline similar volume was taken as other formulations. Thrombosis was induced after 2h of the injection by the topical treatment of $FeCl_3$ (20% w/v) soaked with Whatman filter paper (2 mm × 1

mm) to the same carotid artery in front of the cannulation point. Before the $FeCl_3$ application, normal blood pressure was recorded for at least 10 min as the initial recording, the data recording setup for $FeCl_3$ model in rats had been shown in **Figure 3.10 B**. Aluminum foil was kept below the artery to avoid the contact of $FeCl_3$ with other tissues, before the application. The time for cessation in blood flow after the application of $FeCl_3$ was noted [196]. After the treatment of the carotid artery with $FeCl_3$, the cessation in blood flow and a 50% fall in blood pressure were determined as the end point of the study. The experiment was performed in the controlled environmental condition of a temperature of around 25 °C.

3.4.8.2. Statistical analysis

The statistical data were obtained using the GraphPad Prism software, and all of the experimental data were expressed as mean ± standard deviation of three experimental data. To compute statistically significant differences, one-way analysis of variance (Tukey's multiple comparison test) and the t-test were used. The level of significance is indicated by ns ($p \geq 0.05$), * ($p < 0.05$), * * ($p < 0.01$), and * ** ($p < 0.001$).

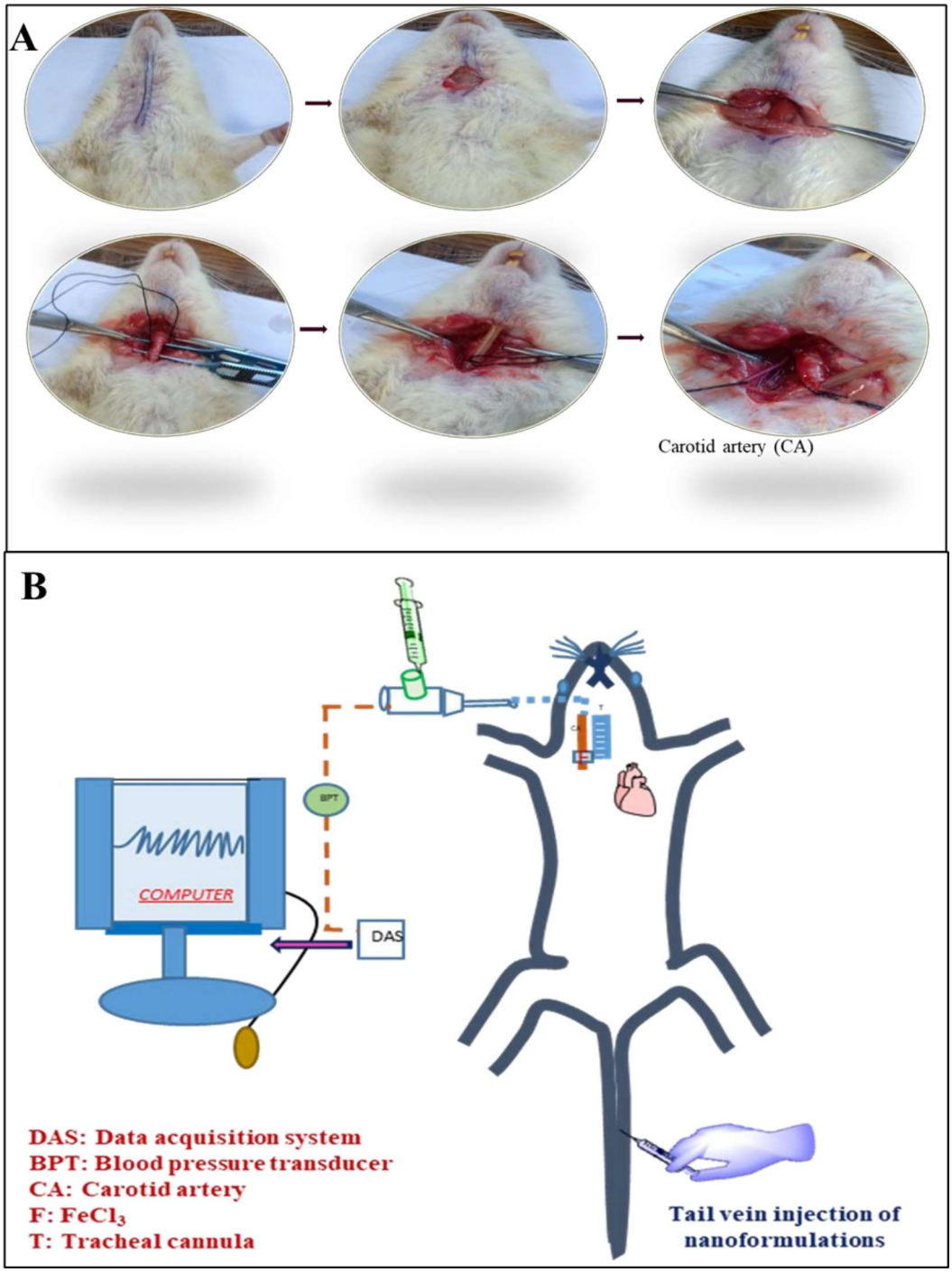

Figure 3.10. A) Surgical steps of $FeCl_3$ model B) Data recording setup for $FeCl_3$ model in rat

3.5. Results and discussion

3.5.1. Formulation optimization by Box-Behnken Design

Table 3.3. Box-Behnken design table with the response values

Batch No.	CTAB (%W/V)	TEOS (mL)	APTES (mL)	Particle Size (nm)	PDI
1	0.625	2.5	0.75	289.2	0.293
2	0.625	3.75	0.5	307.7	0.352
3	0.625	3.75	0.5	307.7	0.339
4	0.25	3.75	0.75	358	0.509
5	1	3.75	0.75	545.3	0.696
6	0.625	5	0.25	346.2	0.5
7	0.625	2.5	0.25	187.7	0.233
8	0.25	2.5	0.5	169.4	0.203
9	0.25	5	0.5	356	0.5
10	0.625	5	0.75	357.3	0.5
11	1	3.75	0.25	378	0.551
12	0.25	3.75	0.25	411.8	0.641
13	1	5	0.5	364.1	0.537
14	0.625	3.75	0.5	307.7	0.323
15	1	2.5	0.5	322.3	0.39

3.5.1.1. Effect on particle size

For all the responses, the quadratic model was selected among various models i.e., linear, 2FI, and cubic. By considering the outcomes of statistical analysis of variance (ANOVA) of R^2 (0.9999), adjusted R^2 (0.9998), predicted R^2 (0.9989), and adeq precision (374.62), the model was analyzed. The predicted R^2 of 0.9989 is in reasonable agreement with the adjusted R^2 of 0.9998; i.e. the difference is less than 0.2. Adeq Precision measures the signal-to-noise ratio and indicates an adequate signal > 4 i.e., desirable. The results demonstrated that the model fit was significant and the lack of fit was non-significant suggesting the suitability of the model. The relationship between the investigated factors

and responses was depicted in **Figure 3.11** in terms of 2D contour plots and 3D surface plots. The polynomial equation generated by BBD showing the effect of different factors on particle size was given as follows:

$Y1 = 307.7 + 39.3125A + 56.875B + 28.2625C - 36.2AB + 55.275AC - 22.6BC + 61.7125A^2 - 66.4625B^2 + 53.8625C^2$

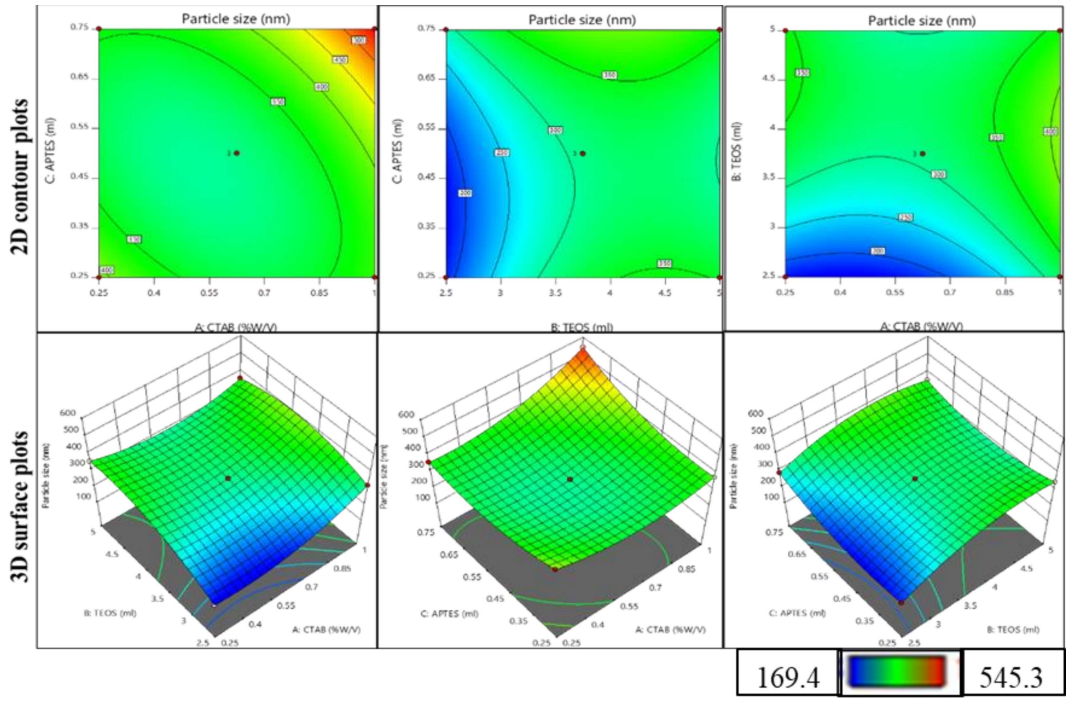

Figure 3.11. The 2D contour plots and 3D surface plots showing the effect of independent variables on particle size

3.5.1.2. Effect on PDI

The BBD study suggested a quadratic model as a best-fit model for the PDI optimization of nanoformulation. The statistical values were noted as R^2 (0.9905), adjusted R^2 (0.9734), predicted R^2 (0.8677), and adeq precision (25.88), after ANOVA analysis. The predicted R^2 of is in reasonable agreement with the adjusted R^2 with a difference of less than 0.2. Adeq precision values were > 4 as advisable. The results demonstrated that the model fit was significant and the lack of fit was non-significant suggesting the suitability of the model. The relationship between the investigated factors and responses was depicted in **Figure**

3.12 in terms of 2D contour plots and 3D surface plots. The polynomial equation generated by BBD showing the effect of different factors on particle size was given as follows:

$Y2= 0.338 + 0.040125A + 0.11475B + 0.009125C -0.0375AB + 0.06925AC -0.015BC + 0.143625 A^2 -0.074125 B^2 + 0.117625C^2$

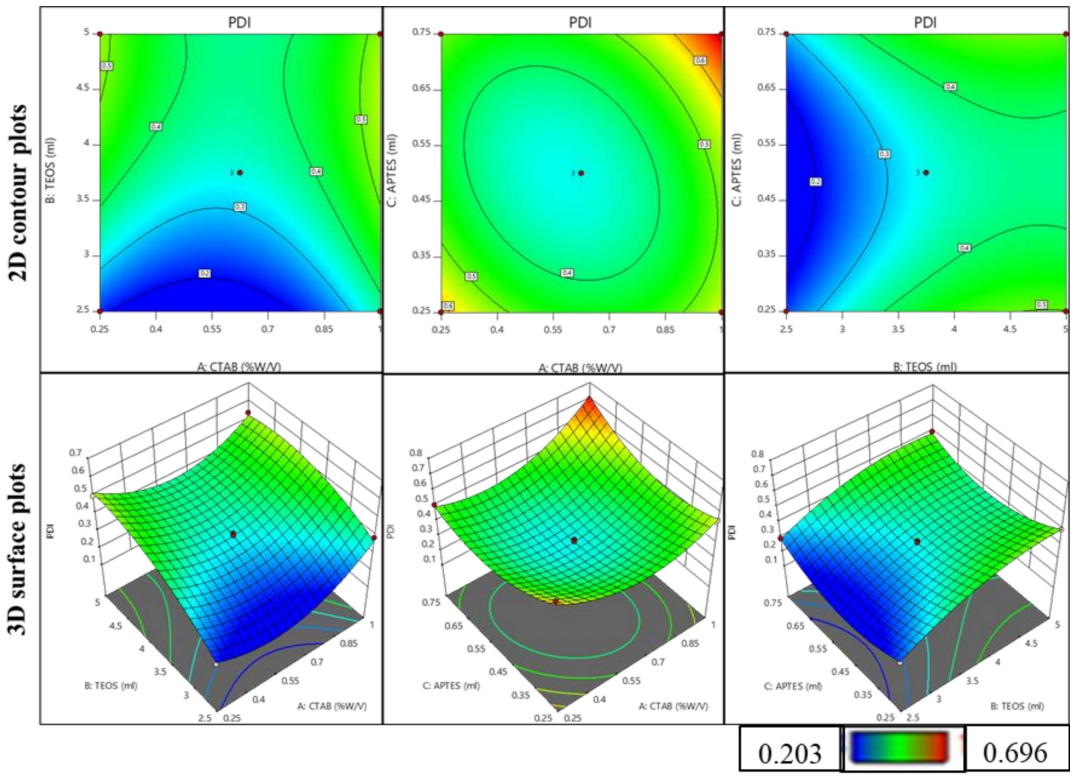

Figure 3.12. The 2D contour plots and 3D surface plots showing the effect of independent variables on PDI

The batch was selected by fixing the independent variables in the range. The response was set as a minimum for particle size and a minimum for PDI. The top 5 suggested batches were experimentally performed and compared with predicted data with a desirability of 1.00. According to experimental results, batch no. 08 was selected for further analysis.

3.5.2. Nanoparticles characterization

3.5.2.1 Size, polydispersity, and zeta potential of nanoparticles

Table 3.4 displays the physicochemical properties of MSN-NH_2 and MSN-ABX. The hydrodynamic diameter of MSN-NH_2 and MSN-ABX were 122.9 ± 5.28 nm and 249.5 ± 2.21 nm respectively. The surface charge of MSN-NH_2 was observed to be + 34.5 ± 3.26

mV, which was diminished following the conjugation with ABX up to − 20.67 ± 1.49 mV indicating their powerful interaction to each other. Therefore analysis of zeta potential demonstrated the positively charged of MSN-NH_2 had been fully occupied by negatively charged ABX [89].

Table 3.4. Particle size, polydispersity, surface charge, and entrapment efficiency values of MSN-NH_2 and MSN-ABX

Type of nanoparticles	Particle Size (Mean ± SD*)	Polydispersity index (Mean ± SD*)	Zeta potential (Mean ± SD*)	Entrapment efficiency (%) for DiD dye (Mean ± SD*)
MSN- NH_2	122.9 ± 5.28	0.242 ± 0.04	+34.5 ± 3.26	-
MSN -ABX	234.5 ± 2.21	0.290± 0.03	-20.67 ± 1.49	-
DiD-MSN-NH_2	129.3 ± 2.61	0.214 ± 0.02	+24.2 ± 2.87	51.12 ± 2.31
DiD-MSN-ABX	237.6 ± 3.31	0.287 ± 0.05	-12.87 ± 2.3	49.35 ± 3.31

*n=3; S.D: standard deviation
DiD-MSN-NH_2: DiD dye loaded mesoporous silica nanoparticles
DiD- MSN-ABX: DiD dye loaded abciximab decorated mesoporous silica nanoparticles

3.5.2.2. TEM analysis

The interior architecture and morphological features of the MSN-NH_2 and MSN-ABX were studied using TEM. **Figure 3.13, A** displays TEM images of nanoparticles in sizes between 100 nm to 200 nm. Individual particles in the images with a 100 nm scale can be interpreted as oval in shape with no noticeable surface flaws. Moreover, as evident from the TEM images, the porous structure of the MSN was clearly observed. The TEM image of MSN-ABX showed a surface coating of ABX as a thin film that confirms the efficient conjugation of ABX on the surface of MSN-NH_2 [197].

3.5.2.3. Scanning electron microscopy

Scanning electron microscopy was used to determine the shape and size of the MSN-NH_2. The images in **Figure 3.13, B**. shows that all of the prepared MSN are monodispersed, spherical, and oval in shape. All the particles were observed under 200 nm of size.

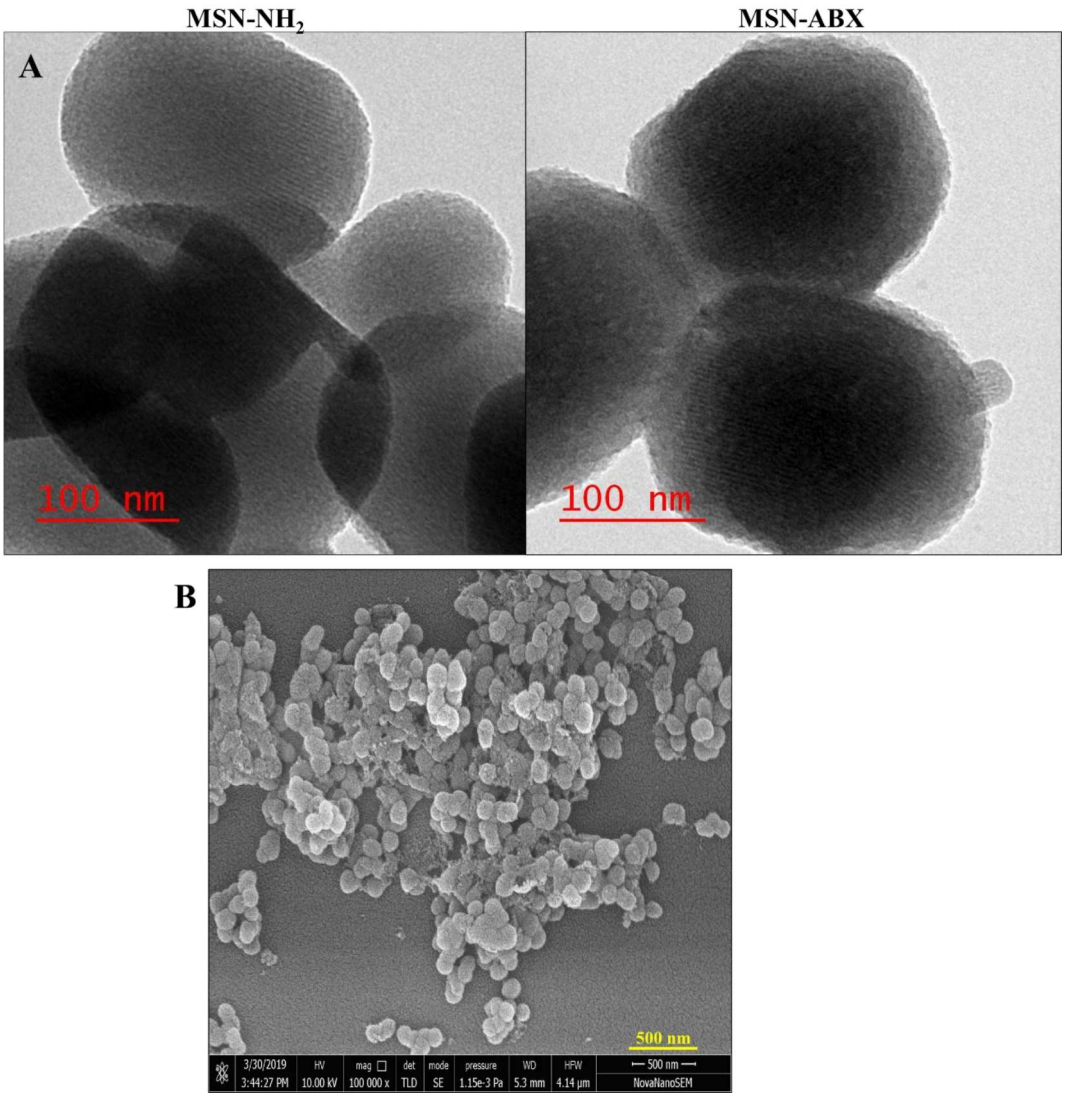

Figure 3.13. A) TEM, images of MSN-NH_2 and MSN-ABX B) SEM image of MSN-NH_2

3.5.2.4. Surface chemistry (XPS survey)

The XPS analysis was used to examine the occurrence of elements over the surface of non-targeted (MSN-NH_2) and MSN-ABX nanoparticles. As presented in **Figure 3.14 A**. the XPS survey revealed the typical peaks of carbon, oxygen, nitrogen, and Silica. The peaks found between the ranges of binding energies 125–140, 100–110, 408–390, 543–523, 296–277 eV were ascribed to SiOx, Si2p, N 1 s, O 1 s and C 1 s. The XPS survey of MSN-NH_2, indicates the percentages of Si2p, N 1 s, O 1 s, and C 1 s were 23.4 %, 1.9 %, 49.7 %, and 24.7 %, respectively., whereas their percentage in XPS survey of MSN-ABX were 6.2 %,

11.1 %, 22.7 % and 59.9 %. As compared to MSN-ABX the atomic percentage of the silica (SiOx and Si2p) on the MSN-NH_2 was significantly higher. The reduction in the atomic percentage of silica in the MSN-ABX, indicated the presence of ABX on its surface. Whereas, the atomic percentage of nitrogen atoms (N 1 s) on ABX decorated nanoparticles significantly increased up to ~6 times. As the molecular formula of ABX contains 551 nitrogen atoms, the increase nitrogen percent in the MSN-ABX supports the successful conjugation of the ABX on the surface of MSN [198].

3.5.2.5. XRD analysis

Figure 3.14 B shows the XRD spectrum of formulated MSN-NH_2. The XRD spectrum revealed well-resolved and intense peak at 23.27◦ 2θ angle, signifies the SiO_2 presence and wide angle XRD pattern at 15–35◦ confirms the existence of MCM-41 or mesoporous silica framework. The observed broad peak denotes the amorphous nature of synthesized MSN-NH_2 that had been reconfirmed with obtained SAED pattern showed in **Figure 3.14 C** [183, 199].

3.5.2.6. TGA study

To further evaluate the thermal stability of prepared MSN-NH_2 in terms of weight change, TGA analysis was used. TGA plot of MSN-NH_2 was indicated in **Figure 3.14 D**, the primary decline in mass of the sample may be due to the loss of physically adsorbed water content and the second decline in mass shows the degradation of products. The 9.72% of initial weight loss was observed due to loss of moisture content in the range of 25 to 120^oC. Then, between 160-340°C there was a gradual loss of weight (17.30%) due to the loss of hydroxyl group. Weight loss was observed in only one decline phase in a progressive manner after 360^oC by the loss of ionic liquid. TGA plot showed the 76% mass retention of the sample at 800 ^oC. The TGA anlysis confirms the high thermal stability of MSN-NH_2 sample over the range of temperatures.

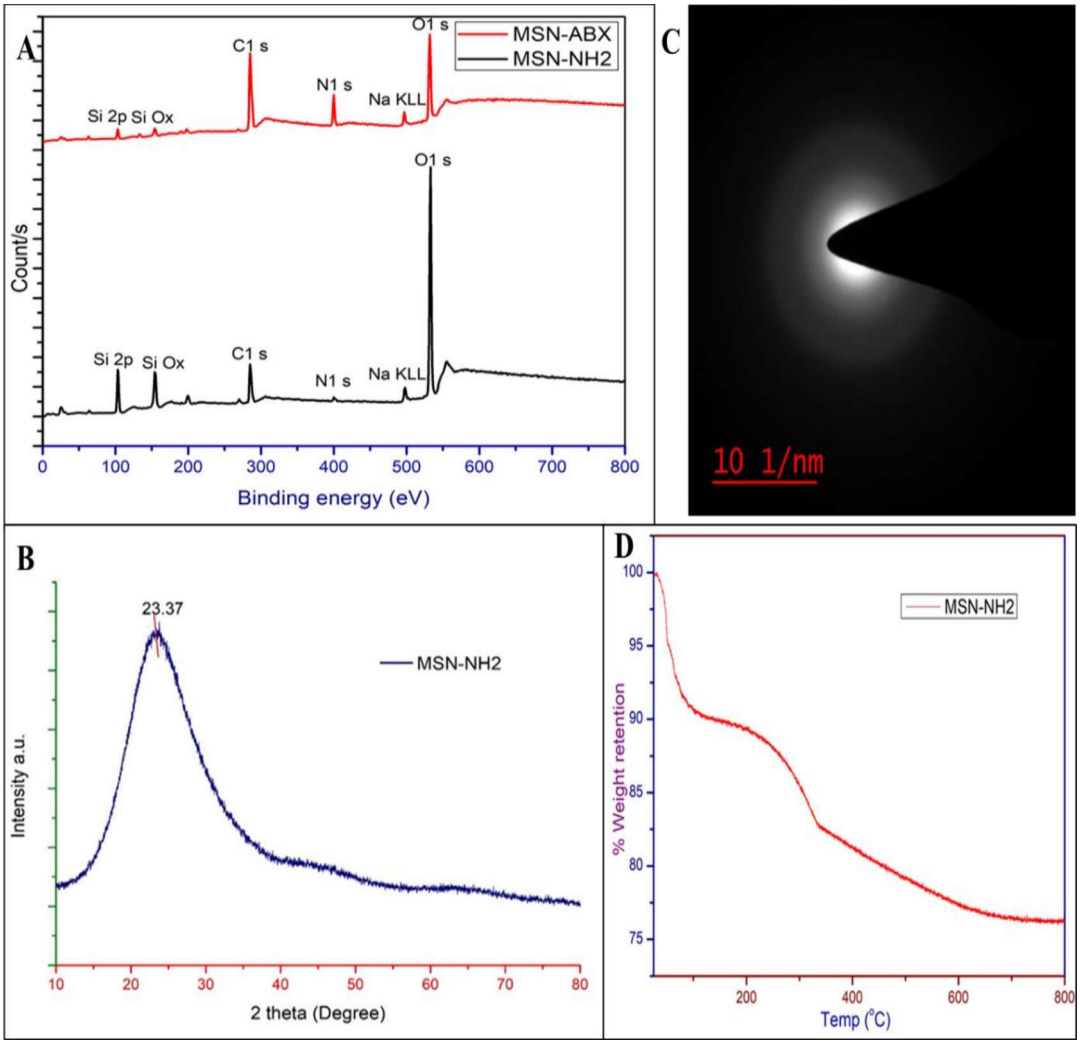

Figure 3.14. (A) XPS survey of MSN-NH_2 and MSN-ABX. B) XRD spectra of MSN-NH_2 C) SAED pattern of MSN-NH_2 D) TGA pattern of MSN-NH_2

3.5.2.7. Degree of ABX conjugation

Bradford assay was used to assess the degree of ABX conjugation to the surface of MSN-NH_2. According to the findings, approximately 67.53 ± 5.81 % of ABX was conjugated on the surface of MSN [200]. The higher ABX conjugation to positively charged MSN-NH_2 suggests the favorable electrostatic interaction between nanoparticle and ABX and is shown to be a prominent candidate for ABX delivery [89].

3.5.2.8. In-vitro analysis

3.5.2.8.1. In-vitro ABX release

The drug release profile of MSN-ABX and ABX marketed injection were studied by the sample separation method for 72 h at pH 7.4 PBS as depicted in **Figure 3.15 A**. The extent of ABX released from the ABX injection and MSN-ABX was found to be 99.8 ± 4.7 %. and 17.61 ± 2.15 in 2 h respectively. After 72 h of drug release study in PBS 7.4, the t 50 % (time of 50 % drug release) of ABX release from the control (ABX injection) and MSN-ABX preparations were about 0.33 h and 18 h respectively. The results revealed that there was a significant decrease in *in-vitro* drug release ($P < 0.05$) in MSN-ABX than clinical ABX injection which signifies the sustained release kinetics of MSN-ABX. The maximum release observed for MSN-ABX was 76.85 ± 0.81 % in 72 h, which is useful since it can avoid the in-vivo degradation or metabolism of the ABX that occurs with clinical abciximab injection [186].

3.5.2.8.2. Blood clot assay

The clot inhibition effect of the ABX clinical injection and MSN-ABX nanoparticles were estimated by performing the blood clot assay. Both ABX and MSN-ABX nanoparticles showed significant reduction ($P < 0.05$) 48.07 ± 5.10 % and 66.33 ± 5.23 % respectively in the blood clot formation as compared to saline control and 51.29 ± 4.41 % and 70.78 ± 2.54 % reduction in the blood clot formation as compare MSN-NH_2 has been shown in **Figure 3.15 B**. The observed significant difference of values between MSN-ABX and ABX injection was due to the uniform distribution of ABX on the surface of MSN that provides an expanded surface area to interact GPIIb/IIIa receptors as compared to free ABX that present in cluster form with the least interaction [188]. However, in relation to an *in-vitro* release study of blood clot assay, it was shown MSN-ABX at a ~ 11 fold lower dose exhibits better inhibition of clot formation than ABX injection in an hour.

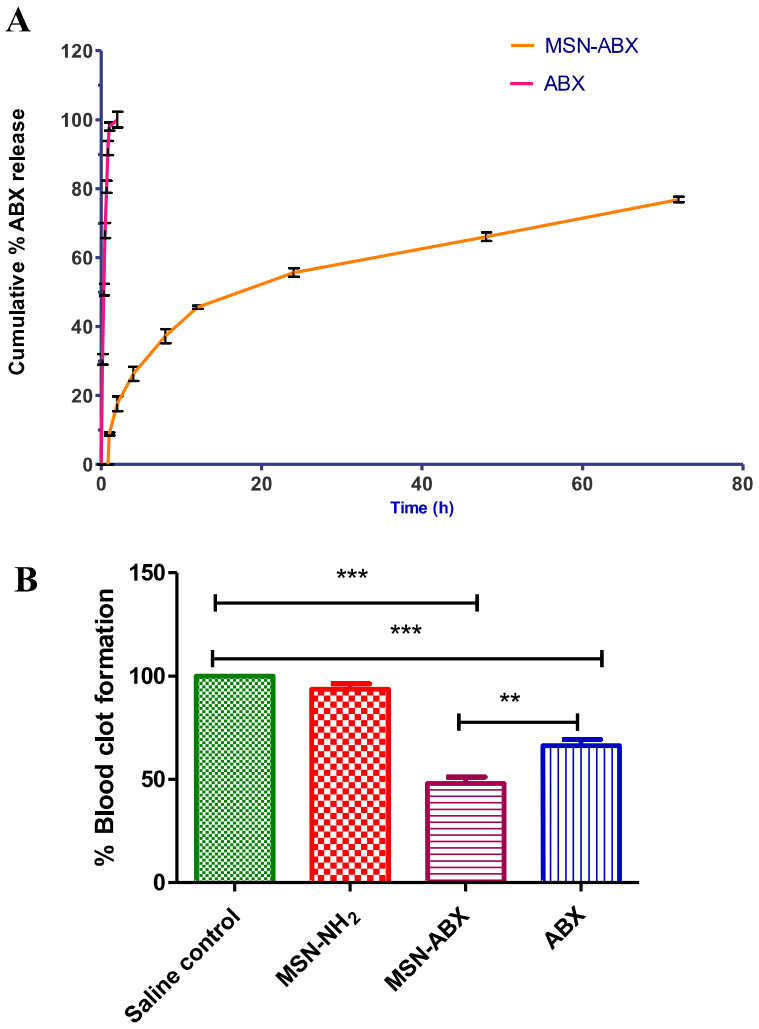

Figure 3.15. (A) Graphical representation of *in-vitro* drug release study of prepared MSN-ABX (solid orange line) as compared to ABX injection (solid pink line). (B) Positive saline control, MSN-NH_2, MSN-ABX, and negative control (ABX) were incubated with freshly collected human blood. *In-vitro* antithrombotic effect of prepared formulation in terms of weight of formed blood clot has been presented. Each of the value was presented in mean ± S.D of three independent investigations. A significant ($P<0.05$) change in clot formation has been observed

3.5.2.9. In-vitro clot targeting efficiency

3.5.2.9.1. In-vitro platelet binding assay by imaging through photon imager optima

In-vitro clot targeting efficiency of MSN-ABX towards activated platelets was determined by imaging system photon imager optima. The fluorescent intensity of the redispersed platelets in PBS treated with DiD-MSN-NH_2 and DiD-MSN-ABX was observed by the

imaging system and respective ROI (Radiance in p/sec/cm2/Sr) data were measured, which was 3.57 × 10^3 ± 1.65 and 11.4 × 10^3 ± 2.67 respectively (**Figure 3.16 A**). The vial containing comparable concentrations of DiD dye that had been loaded in the formulations, showed no fluorescence, indicating that there were no interactions between the dye solution and the platelets. Whereas the platelets treated with DiD-MSN-ABX exhibited a significantly higher intensity ($P < 0.05$) compared to DiD-MSN-NH_2. However, platelets treated with DiD-MSN-NH_2 also showed considerably higher intensity than platelets treated with saline control (P 0.05) which can be interpreted by the interaction (electrostatic) between DiD-MSN-ABX and GP IIb / IIIa receptor present over the membrane of activated platelets. Finally, before treatment with activated platelets, the fluorescent intensity of the standard DiD solution was measured and normalized with the entrapped DiD dye in the formulations, which was used as a positive control to compare the percentage intensity of DiD-MSN-NH_2 and DiD-MSN-ABX, as shown in **Figure 3.16 B and B.1**

3.5.2.9.2. Image-J analysis of CLSM images

The extent of red channels in fluorescent images of activated platelets after treatment was used to estimate the *in-vitro* clot targeting efficacy of DiD dye, MSN-NH_2, and MSN-ABX towards activated platelets. The red channels of fluorescent images were quantified using Image-J software. The proportion of dark area was calculated when the fluorescent images were transformed into binary white and black images. The DiD-MSN-ABX treated activated platelets showed a significantly increased fluorescent intensity ($P < 0.05$) as compared to DiD dye and DiD-MSN-NH_2 treated which confirms the specific interactions of ABX of the MSN with the GPIIb/IIIa receptor has been presented in **Figure 3.16 A and A.1**. Moreover, the platelets treated with DiD-MSN-NH_2 also showed increased fluorescent

intensity (not significant as compare to DiD dye treated) possibly due to the electrostatic interactions as it has a positive surface charge.

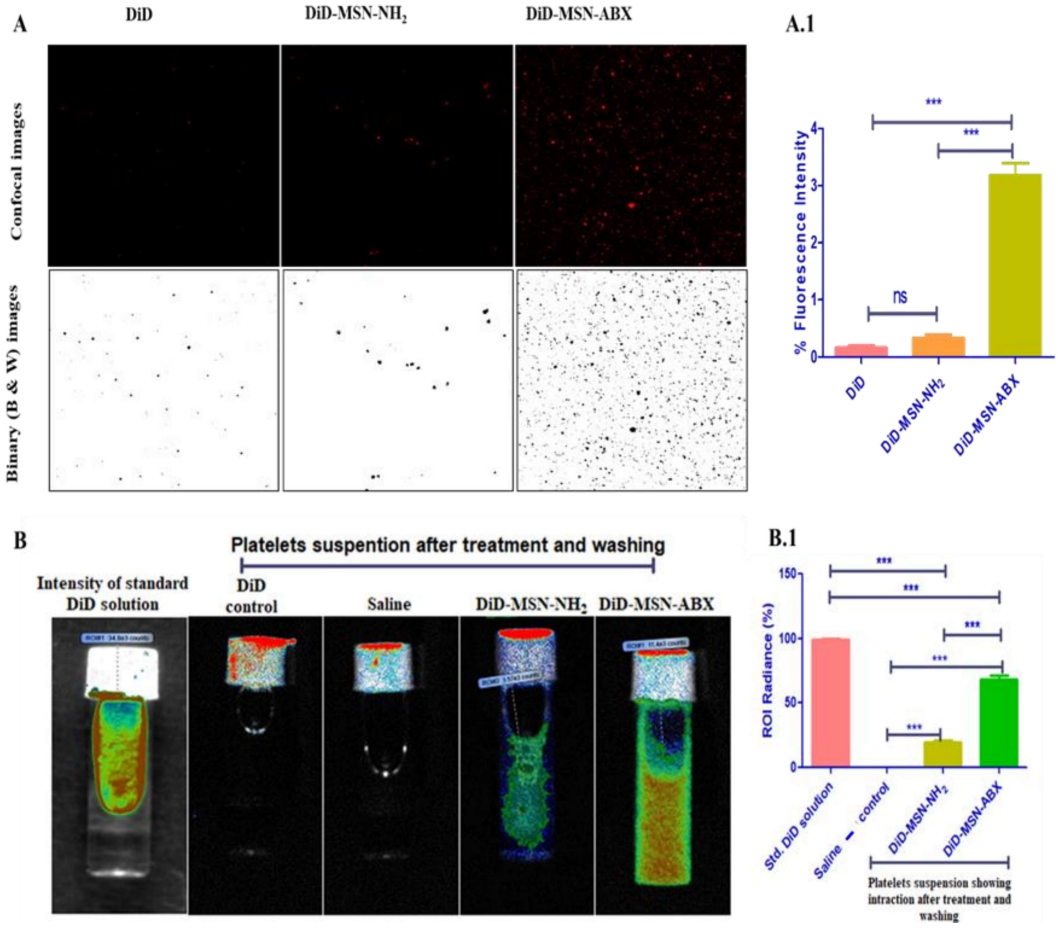

Figure 3.16. (A) Confocal laser scanning microscopic images and binary black and white images (converted by the image-J software) of activated platelets treated with DiD dye, DiD-MSN-NH_2 and DiD-MSN-ABX. (A.1) The percentage fluorescent intensity of red channels presents in their corresponding microscopic images. (B) Fluorescent images of vials containing standard DiD dye solution and washed activated platelets after the treatment with DiD dye control, saline, DiD-MSN-NH_2 and DiD-MSN-ABX obtained by photon imager optima imaging sysytem. (B.1) Bar graph demonstrating the % interaction of DiD-MSN-NH_2 and DiD-MSN-ABX as compared to DiD control

3.5.2.10 In-vitro safety assessment

3.5.2.10.1. Blood Smear

The light microscopic images (**Figure 3.17 B**) of the blood smear treated with the ABX, MSN-NH_2, and MSN-ABX did not demonstrate any significant change in the morphology of the blood cells.

3.5.2.10.2. Hemolytic Assay

The safety of the non-targeted, abciximab decorated MSN and abciximab clinical injection in the blood was assessed by the hemolytic assay. The percent hemolysis of the abciximab injection, non-targeted, and targeted MSN are 0.085 ± 0.014 %, 0.024 ± 0.009 %, and 0.022 ± 0.011 %. The results (**Figure 3.17 A)** demonstrated that ABX, non-targeted, and the ABX decorated MSN are non-hemolytic to human blood.

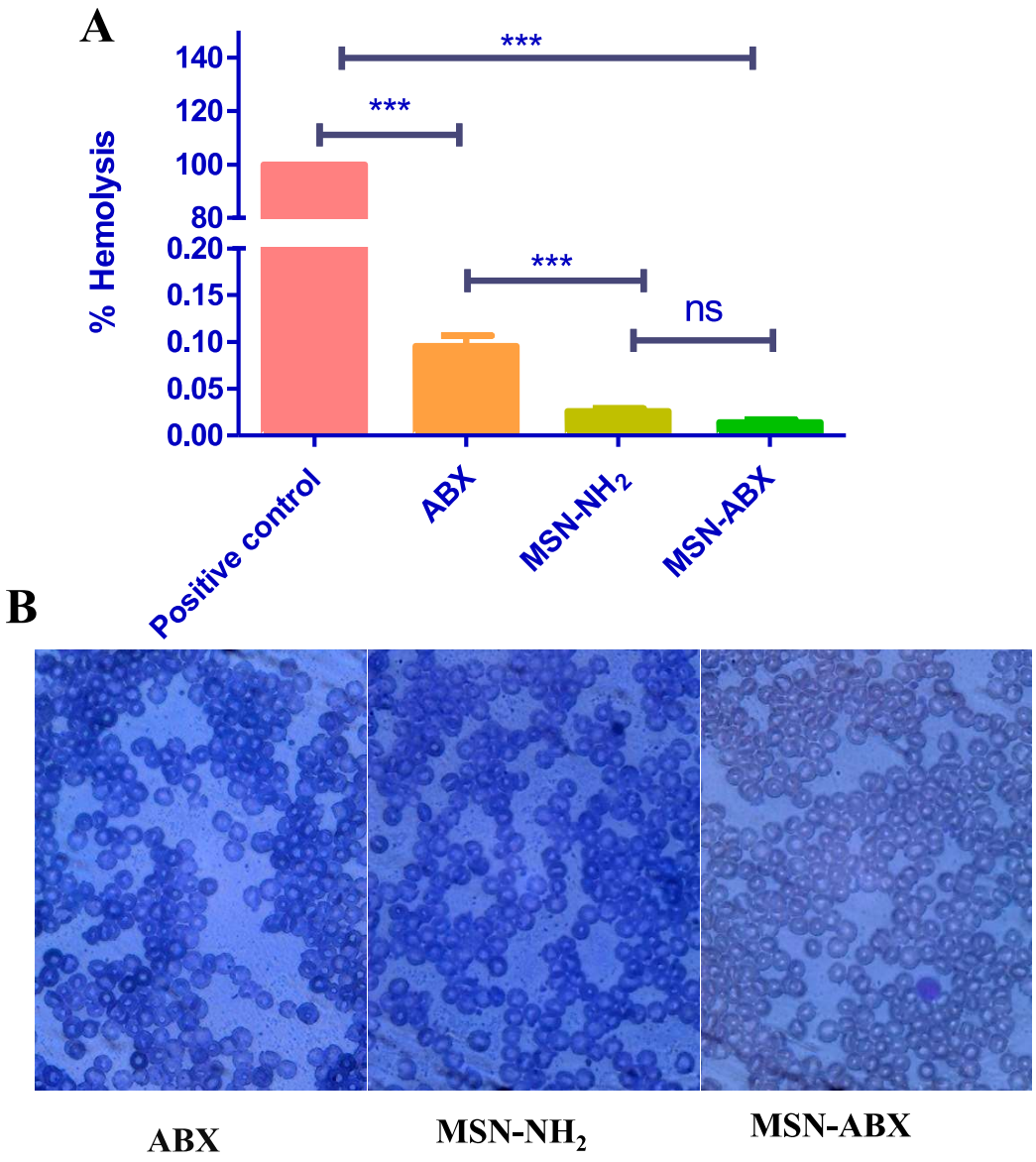

Figure 3.17. (A) Bar graph showing % hemolysis and (B) bright microscopic images (10 X) of human blood treated with ABX injection, MSN-NH_2, and MSN-ABX

3.5.2.11. In-vivo studies

3.5.2.11.1. Tail bleeding assay

This assay has been widely utilized as an *in-vivo* approach to assessing the bleeding characteristics of antithrombotic drugs and drug products. In this investigation, the bleeding time was evaluated after tail vein injection in mice. The bleeding time for saline, ABX, and MSN-ABX were noted as 81.66±5.79, 113.66±5.31, and 117.33±4.91 sec respectively after 1 h of the injection. The method and bar graph of comparative bleeding time was presented in **Figures 3.18 A.** From the above mentioned results, it was concluded that ABX and MSN-ABX showed no significantly different bleeding time that corresponds to their specificity towards the thrombotic event and enhanced antithrombotic potential *in-vivo* without increasing bleeding risk. However, as compared to saline, ABX containing groups presented a significant increase in bleeding time.

3.5.2.11.2. Blood clotting time study

The clotting time is defined as the time required to generate thrombin when bleeding occurs at the site of the injury. The clotting time for saline, ABX, and MSN-ABX were noted as 121.00±8.04, 138.14±6.01, and 135.66±8.40 sec respectively after 1 h of the intravenous injection. The bar graph representing comparative clotting time was depicted in **Figure 3.18 B**. In comparison to saline control, other formulations showed a nonsignificant increase in clotting time which suggests the non interactive nature MSN-ABX to clotting enzymes and has proven as a good nanocarrier to deliver ABX.

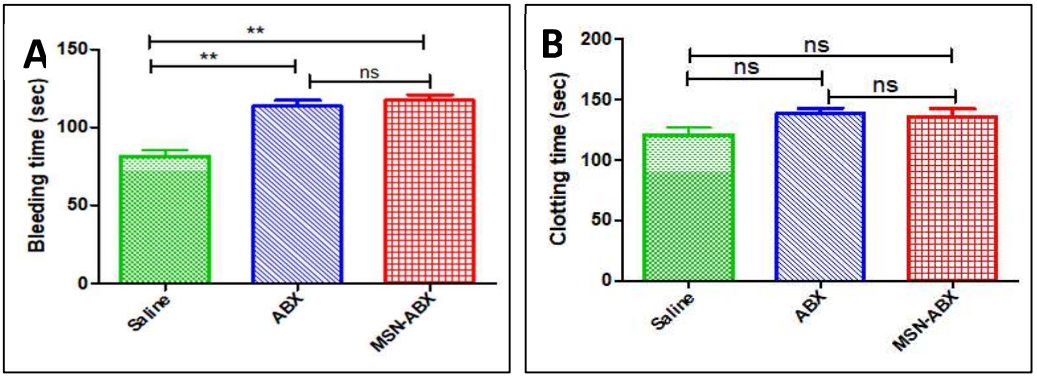

Figure 3.18. Bar graph depicting the A) bleeding time B) clotting time in sec

3.5.2.11.3. In-vivo $FeCl_3$ induced model for thrombus formation by B.P. measurement

Initially, after the right carotid artery cannulation, Whatmann paper saturated with 20% $FeCl_3$ solution was applied to the carotid artery in rats, till the complete occlusion. Time taken to decline by 50% in B.P (T_{50}) was measured with the help AD instrument. The T_{50} for saline, ABX, and MSN-ABX were observed as 2.90±0.40, 7.01±1.43, and 14.16±1.34 min, respectively, depicted in **Figure 3.19 A and B.** As compared to saline, and ABX the MSN-ABX showed a significantly higher value (time taken for clot formation) presented in **Table 3.5**. The MSN-ABX showed a 2 times higher value as compared to ABX confirming its superior antithrombotic potential over conventional formulation.

Table 3.5. Effect of various formulations on blood pressure in $FeCl_3$ induced blockage in CA.

Group name	B.P before treatment (mm of Hg) (Mean ± SD#)	B.P after treatment (mm of Hg) (Mean ± SD#)	Avg time taken to fall in 50% B.P. (min) (Mean ± SD#)
Saline	87.33 ± 15.92	43.66 ± 7.96	2.90±0.40
ABX control	90.00 ± 07.87	45.50 ± 3.93	7.00±1.43* (P<0.05)
MSN-ABX	86.66 ± 11.67	43.33 ± 5.83	14.16±1.13***(P<0.001)

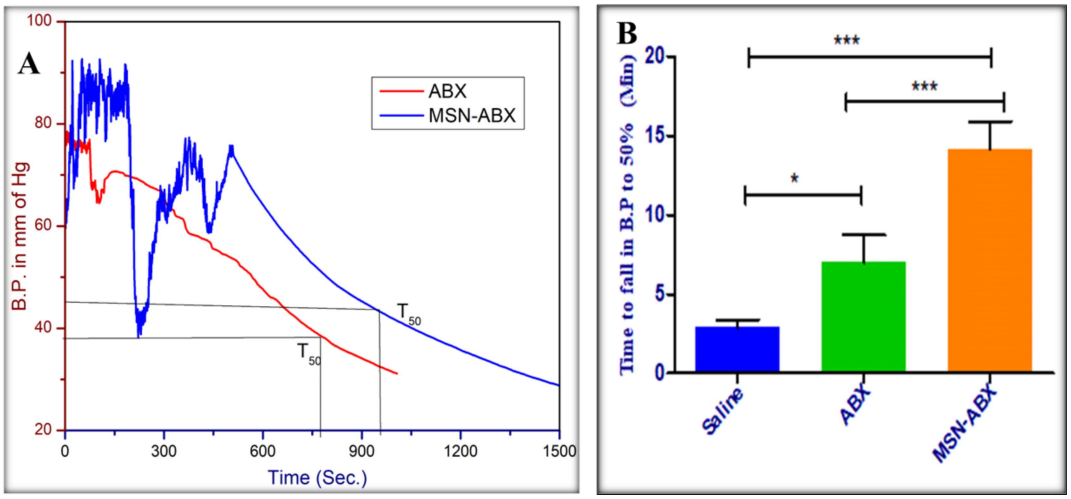

Figure 3.19. A) Line graph showing the original B.P. measurements B) Bar diagram represents the time of 50% fall in BP in CA (ns ($p \geq 0.05$), * ($p < 0.05$), ** ($p < 0.01$), and *** ($p < 0.001$)

3.6. Conclusion

The clinical injection of ABX is used widely for the prophylaxis management of thrombosis, myocardial infarction, atherosclerosis, and stroke. Although it is one of the most widely used antiplatelet drugs, it has a much shorter biological half-life and has shown dose-related side effects such as a high risk of bleeding. Therefore, there is a need for the development of advanced drug delivery system which can enhance its half-life and reduce dose related side effects. In this work, we have developed the MSN coated with the ABX for improved antithrombotic activity. The ABX decorated MSN was prepared by electrostatic interactions between the amino factionalized nanoparticles and ABX injection. All the physicochemical parameters including particle size, zeta potential, surface charge, thermal stability, degree of conjugation, and morphology analysis (SEM, TEM, TGA) examined. The average particle size, polydispersity, and surface charge of all the batches of nanoparticle preparation were in the acceptable range. The XPS survey explained the presence of ABX on the surface of MSN-NH_2. The degree of conjugation of ABX to the surface of amino-functionalized MSN was 67.53 ± 5.81 % as determined by the Bradford test. The *in-vitro* targeting efficiency of the ABX decorated MSN towards activated

platelets was determined by confocal laser scanning microscopy and the spectrum obtained through a photon imager optima imaging system. Their results showed that platelets treated with DiD-MSN-ABX exhibited the highest intensity compared to the DiD dye and the negative control. The safety of the formulations in human blood was evaluated by the hemolysis assay and the results showed that 0.085 ± 0.014 %, 0.024 ± 0.009 %, and 0.022 ± 0.011 % hemolysis of ABX injection, MSN-NH_2, and MSN-ABX respectively. In addition, the safety assessment was determined by observing the morphology of the blood cells by making a blood smear after incubation with the formulations and the results showed no significant change in the morphology of the cells. At last, the *in-vitro* assessment of the formulation was determined by blood clot assay. The blood samples treated with ABX injection as well as the MSN-ABX successfully inhibited the clot formation to 48.07 ± 5.10 and 66.33 ± 5.23 % respectively as compared to saline control *in-vitro*. As MSN-ABX has an affinity for activated platelets and is stable under physiological conditions, therefore its role in enhancing antithrombotic activity has been successfully demonstrated. However, the *in-vivo* studies demonstrated no significant change in bleeding and clotting time when formulated as an MSN-ABX. Moreover, the $FeCl_3$-induced thrombosis model in Sprague Dawley rats suggested 2 times greater antithrombotic potential of MSN-ABX as compared to ABX injection when administered via the tail vein. These nanoparticles have shown promising preclinical outcomes and may be translated into an effective ABX delivery tool as a potential clinical alternative with a higher safety reliance. However, clinical trials must be carried out to confirm its potency in the inhibition of platelet aggregation in individuals. The major concerns involved related to side effects like hemorrhage, biodegradability, and toxicity should also be addressed prior to its regulatory approval for clinical usage. Graphical illustration of ABX coated MSN for antithrombotic therapy had been depicted in **Figure 3.20**.

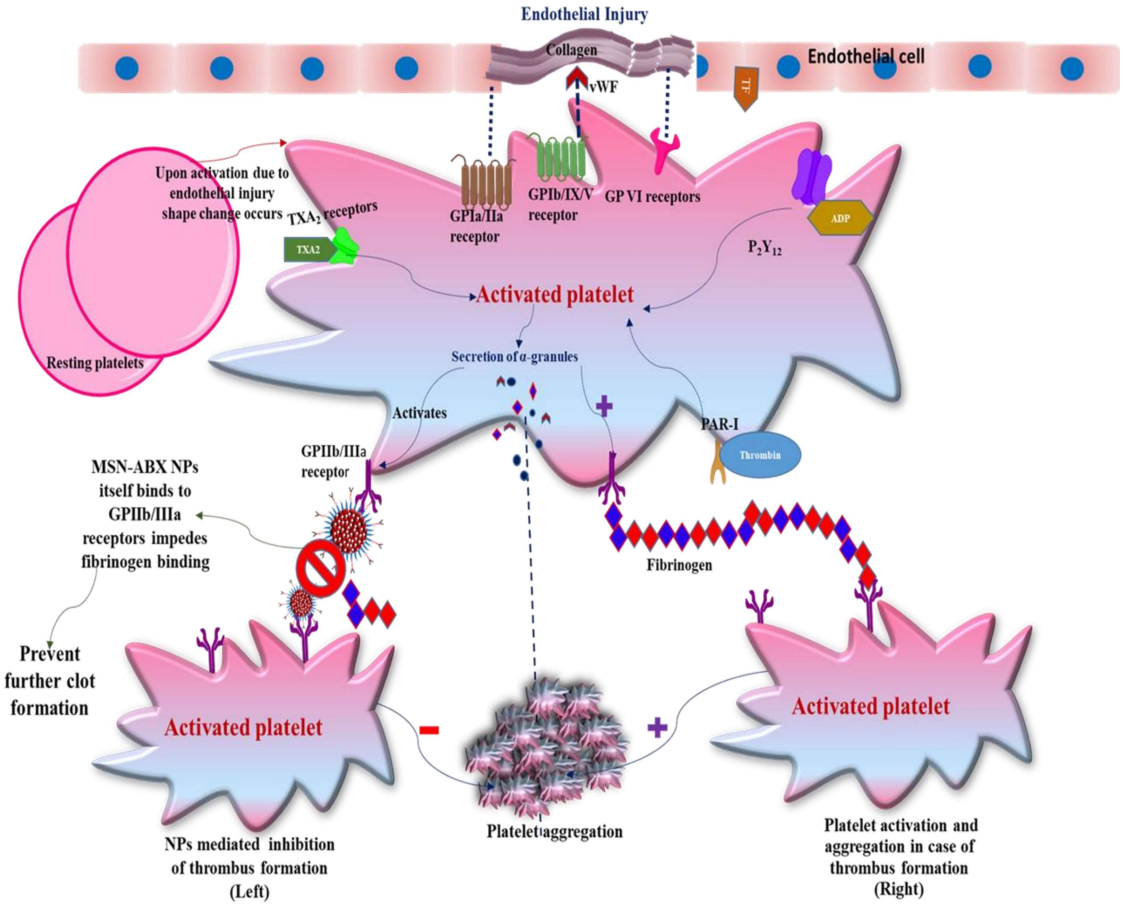

Figure 3.20. Graphical illustration of ABX coated MSN for antithrombotic therapy